SSC24-WIII-06

Design, Characterization, and Testing of HERT, a Miniaturized High-Energy-Resolution Relativistic Electron Telescope for CubeSats

Hong Zhao, Will Teague
Auburn University
380 Duncan Drive, Auburn, AL 36849; 334-844-4628
zzh0054@auburn.edu

Lauren Blum, Xinlin Li, Jared Cantilina, Will Edgar, Tyler Bishop
LASP, University of Colorado Boulder
1234 Innovation Drive, Boulder, CO 80303

Patricio Ramos
Blueshift, LLC DBA Outward Technologies
155 Commerce St, Broomfield, CO 80020

Skyler Krantz
NASA Johnson Space Center
2101 E NASA Pkwy, Houston, TX 77058

ABSTRACT

Earth's outer radiation belt is filled with relativistic electrons in the MeV energy range and above. These highly energetic electrons pose significant threats to avionics and humans in space, and understanding their dynamics has been an urgent need. As CubeSats increasingly play a more prominent role by executing missions at a far lower cost, they become ideal vehicles for conducting such scientific investigations. The miniaturized High-Energy-Resolution relativistic electron Telescope (HERT) is a compact telescope designed for a 6U CubeSat mission in a geosynchronous transfer orbit (GTO). HERT aims to provide high-energy-resolution (dE/E < 12%) measurements of 1 – 7 MeV electrons at GTO. These measurements will enable a novel method to differentiate the two main acceleration mechanisms, inward radial transport and local acceleration, and solve the longstanding question of how electrons in the Earth's radiation belts are accelerated to relativistic energies. Building upon the heritage of the Relativistic Electron Proton Telescope (REPT) instrument on the Van Allen Probes and the REPTile-2 instrument on CIRBE, HERT is comprised of a stack of nine solid-state silicon detectors in a telescope configuration with a beryllium window to block lower energy electrons and a tantalum collimator to enforce the required FOV (33°). The instrument responses were investigated using Geant4 simulations, and the results project HERT to have a nominal energy resolution of ~5% for 1.5 – 3 MeV electrons and < ~12% for other core energy channels. Radiation testing has been conducted with a Cobalt-60 source, and the results suggest that HERT electronics can sustain a total ionizing dose of ~65 krad, meeting the instrument performance requirement in a GTO. Random vibration simulations have also been conducted, which suggest that HERT's reaction stresses and displacements are within a significant safety factor relative to yield strength from each component. Bench testing with muons and an SR-90/Y-90 radioactive source is ongoing to test HERT's performance. With a high energy resolution and a miniaturized design, HERT will greatly advance the quantitative understanding of relativistic electron acceleration in the outer radiation belt.

INTRODUCTION

The radiation belts, consisting of the outer and inner belts, are the regions in Earth's inner magnetosphere where energetic charged particles are geomagnetically trapped, azimuthally drifting around the Earth. They present a hazardous radiative environment for spacecraft operating within. Thus, understanding the dynamics of radiation belt electrons is of significant scientific interest and practical needs. Specifically, the outer radiation belt is occupied with relativistic electrons of energies from 100s of keV to >10 MeV. It is highly dynamic, and energetic electrons in the outer belt often exhibit significant acceleration and loss.

Since the discovery of the radiation belts in 1958, a fundamental unanswered question has been how radiation belt electrons are accelerated to such high energies. Two main acceleration mechanisms have been

proposed: inward radial transport, which accelerates electrons by transporting them Earthward to places with stronger magnetic fields while conserving their magnetic moments, and local acceleration, which accelerates lower-energy electrons to higher energies in situ in the heart of the outer belt.[1-5] However, the relative importance of the two acceleration mechanisms has not been fully understood because of 1) sparse in-situ observations between the altitude of ~5.8 R_E and geosynchronous orbit (GEO) despite the drastic changes in >MeV electron concentration over this region, and 2) difficulties in disentangling the effect of the two acceleration mechanisms.

Recently, a novel method has been proposed to quantify the radial transport rate based on a critical fact of radial transport that has been overlooked for years: radial transport produces drift-periodic oscillations in the electron flux at the electron drift frequency[6,7]. These drift-periodic flux oscillations are the microscopic behavior and a unique identifier of radial transport, since another mechanism, local acceleration, causes flux variations at the electron cyclotron frequency which is much faster than a typical electron detector's response. Combining these drift-periodic flux oscillation observations with simulations, the radial transport rate can be derived, the effect of radial transport on radiation belt electrons can be accurately quantified, and the effects of the two major acceleration mechanisms can be disentangled.

This novel method requires sufficient energy resolution of electron flux measurements since electrons of different energies drift at different speeds, and only with sufficient energy resolution can the drift-periodic flux oscillations of electrons of different energies be clearly disentangled. However, there are currently no available in-situ measurements with a sufficient energy resolution of >1 MeV electrons, the core population of the radiation belt, to clearly discern the drift-periodic flux oscillations.

Thus, to understand and quantify the acceleration of relativistic electrons in the outer radiation belt, we develop the High-Energy-Resolution relativistic electron Telescope, HERT, aiming for the geosynchronous transfer orbit (GTO). Since SmallSats and CubeSats have been proven to be viable platforms for science and technology, HERT is developed as the sole science payload for a 6U CubeSat. The instrument development project is sponsored by the NASA H-TIDeS program. Providing high-energy-resolution relativistic electron measurements in the outer radiation belt with a miniaturized design, HERT will greatly advance the quantitative understanding of the radiation belt electron acceleration.

SCIENCE GOAL AND OBJECTIVES

HERT's science goal is to understand radiation belt electron dynamics. Two specific science objectives have been identified: 1) understanding the energy-dependent acceleration of relativistic electrons in the entire outer radiation belt, and 2) quantifying the contribution of radial transport to the energy-dependent acceleration of outer radiation belt electron core populations. To achieve these science objectives, HERT is required to measure 1 – 7 MeV electron fluxes with a high energy resolution (dE/E < 12%) and radial flux profiles throughout the entire outer radiation belt onboard a CubeSat at GTO.

INSTRUMENT DESIGN AND CHARACTERIZATION

HERT is a compact telescope designed for a 6U CubeSat mission to measure 1-7 MeV electron differential fluxes with a high energy resolution. HERT is built on the heritage of the Relativistic Electron Proton Telescope (REPT)[8,9] on the Van Allen Probes[10,11], the Relativistic Electron Proton Telescope integrated little experiment (REPTile) instrument on the Colorado Student Space Weather Experiment (CSSWE)[12], and the REPTile-2 instrument[13] on the Colorado Inner Radiation Belt Experiment (CIRBE)[14,15]. With simplified electronics and an updated detector design, HERT can provide measurements of 1 – 7 MeV electrons with higher energy resolution (~5% at 1.5 – 3 MeV and <12% otherwise) at a much smaller SWaP (2.2U/3kg/4W) compared to REPT.

HERT consists of three subsystems: sensor head, electrical subsystem, and mechanical subsystem. Its sensor head comprises nine solid-state silicon detectors in a telescope-type configuration. The first detector has a diameter of 20 mm, while the rest have a diameter of 40 mm. Tungsten sheets form a 5 mm stack providing shielding at the front and back of the detector stack, and a 4 mm thick tungsten epoxy chamber comprises the shielding surrounding the detector stack, limiting non-field-of-view (FOV) particles from reaching the detectors. Sheets and tungsten-epoxy instead of solid tungsten are used to ensure that HERT meets the orbital debris requirements. A tantalum collimator with five knife-edged baffles with openings of 18 mm enforces the desired FOV of ~33°. A 1.5 mm thick Beryllium window at the end of the collimator acts as a high-pass filter and prevents low-energy particles (≤ ~0.5 MeV) from depositing sufficient energy (≥ 0.1 MeV) in the detector stack. Figure 1 shows pictures of HERT's sensor head and the whole assembly.

Figure 1 (Top) HERT sensor head; (bottom) HERT whole assembly.

HERT determines the incident energy of electrons by measuring the deposited energy in the detector stack. As energetic charged particles pass through detectors, they deposit energy at detectors through electromagnetic interactions at a rate inversely proportional to the particle kinetic energy. Each detector is provided with an optimized bias voltage and has independent charge sensitive amplifiers (CSA) (except for the 7th and 8th detectors, which are wired together). The ~300V bias voltage permits prompt collection of charges liberated in the detector, and the CSAs convert the collected charges into proportional voltage pulses. With minimal signal conditioning and pulse height analysis (PHA), the charge pulses are measured by continuously sampling 14-bit Analog to Digital Converters (ADC). The 14-bit resolution and 50ns sampling cadence (20MSPS) resolve pulse rising and trailing features supporting the FPGA based baseline tracking and PHA measurements. Using PHA data from the ensemble detector stack, evaluated against a configurable set of identification parameters, the FPGA classifies each particle event by energy. The count of energetic electrons by energy bin is collected and reported.

HERT is designed with 40 electron energy channels, with 38 core channels of nominal energies from 1 to 7 MeV and 2 bonus channels providing lower energy electron measurements down to ~0.6 MeV. Figure 2 shows the geometric factors of HERT's energy channels as a function of the electron incident energy. The geometric factors are calculated using Geant4 simulations with 100 million incident electrons, shooting from a spherical cap particle source [16] with randomized initial energy between 0 and 8 MeV. The nominal energy of each energy channel is then determined by bow-tie analysis using geometric factors derived from Geant4 simulations, and the channel width is identified as the full-width-half-maximum of each geometric factor curve. The energy resolution, defined as the channel width divided by the channel's nominal energy, is found to be below ~12% for each core energy channel. For energy channels with a nominal energy between ~1.5 and 3 MeV, the energy resolution can reach as low as ~5%. The count rate estimates of each detector and each energy channel show that 95th percentiles of AE9 fluxes will not saturate the detectors, and each energy channel has sufficient counting statistics with 1s measurement cadence using 50th percentiles of AE9 fluxes near the center of the outer belt. Under lower flux conditions, such as during geomagnetically quiet times, the counts can be summed over multiple time bins on the ground to provide sufficient counting statistics while still fulfilling the measurement cadence requirement (<1 min). Detailed descriptions of HERT sensor head design and characterization based on Geant4 simulations can also be found in Krantz et al. (2023)[16].

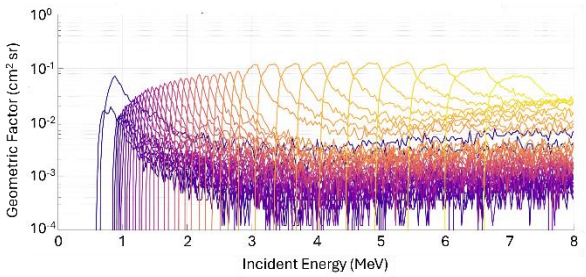

Figure 2 HERT's geometric factor by energy channel as a function of electron incident energy.

INSTRUMENT TESTING

Radiation Testing

Another challenge for HERT is to survive the harsh radiation environment at GTO. HERT's performance requirement includes sustaining at least 50 krad total ionizing dose (TID). HERT's electronics are primarily based on the heritage of REPTile-2. HERT uses the

Kintex-7 FPGA (free from destructive latch-ups), which has been tested and survived 100 krad TID, TMR's serial configuration flash, MRAM for nonvolatile storage, and up to 8GB of radiation-hardened NAND flash for data storage. The CSAs have been upgraded to the rad-hard version that can sustain >100 krad TID. The ADC and power boards use tolerant buck converters and ADCs. Radiation testing for HERT's ADC board has been conducted with a Cobalt-60 source at Auburn University to determine the radiation tolerance. Figure 3 shows the HERT's ADC board TID testing setups. The ADC board is connected to the FPGA board and power supply and exposed to the gamma radiation generated by the Cobalt-60 source at a distance of ~40 cm (dose rate of 1 rad/s) while running. A computer is connected to the FPGA board via an RS-422 serial receiver and continuously takes data. The mean and standard deviation in data number (DN) of each channel are recorded during the radiation exposure and analyzed after the test to determine the radiation tolerance of HERT's ADC board. The TID testing is temporarily stopped at ~65 krad due to the failure of the RS-422 chip (for testing diagnostic purposes only and not for the flight instrument) and the flash chips on the FPGA board.

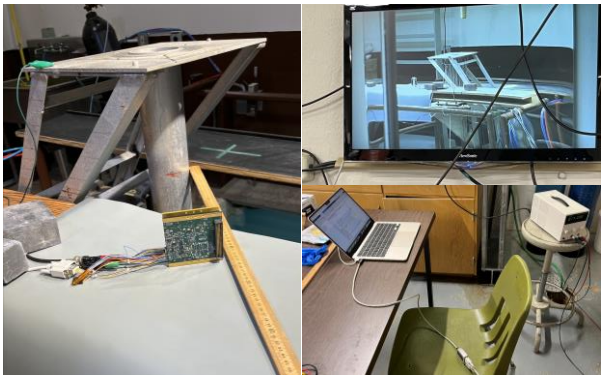

Figure 3 HERT's ADC board TID testing setups. (Left) HERT's ADC and FPGA boards were placed at ~40 cm from the center of the Co-60 radiation source inside the radiation chamber before the exposure; (upper right) HERT's ADC and FPGA boards during the radiation exposure as seen from the monitor outside the radiation chamber; (lower right) HERT electronic boards were connected to the power supply and a computer for continuously collecting data during the radiation exposure.

The HERT's ADC board TID testing results are shown in Figure 4. It shows that the change in the mean DN of each channel over time is very small during radiation exposure. The standard deviations of all channels are less than 3 DN during the whole test, which is much smaller than the expected electronic noises (~30 DN based on REPTile-2 testing results). These results demonstrate a radiation tolerance of HERT's ADC board of > ~65 krad, meeting the performance requirement at a GTO.

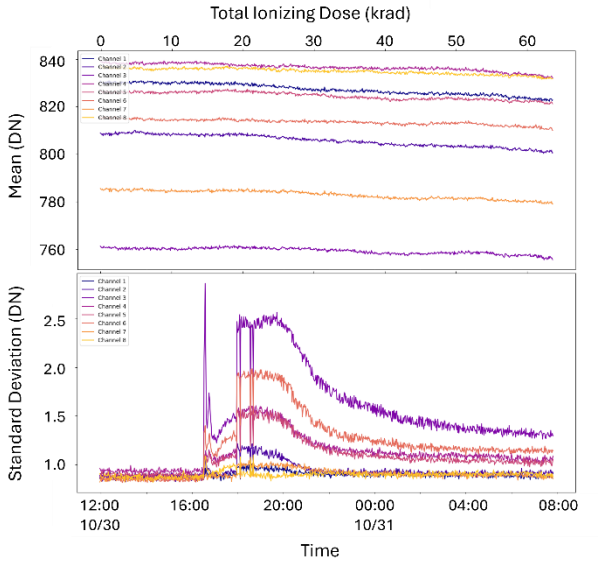

Figure 4 HERT ADC board TID testing results. (Top) Mean and (bottom) standard deviation in data number as a function of time under radiation exposure and the corresponding TID. Each curve corresponds to one channel.

Random Vibration Simulation

Using SolidWorks, random vibration simulations have been conducted for HERT to serve as a preliminary check against the structural integrity and ensure that the instrument can be subjected to a vibrational load where its reaction stresses and displacements are within a significant safety factor of the yield strength from each of the components. Using NASA GEVS 7000, we determine the required base excitation load applied to the mounted instrument. The assumptions made include: 1) the "feet" of HERT are fixed; 2) components that are fastened to each other are bonded; 3) gaps between components are not bonded. Figure 5 shows the setup of HERT's random vibration simulation. The small green arrows indicate the fixed endpoints. The gravity in the simulation is pointing in the Y direction (purple arrow), with which we expect to see the highest displacements and the highest stresses located at the center of the instrument.

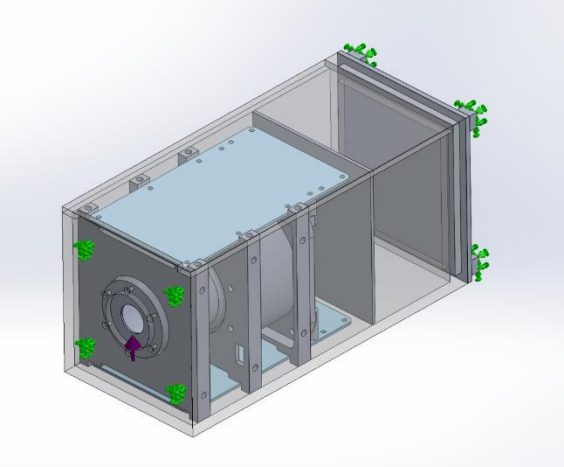

Figure 5 HERT's random vibration simulation setup.

In random vibration simulations, the vibrational load is applied in the X, Y, and Z axes independently. The largest displacements and stresses are observed in the Y-axis excitation (Figure 6), and the CSA boards often show the largest displacements. The simulation results show that average displacements are within ~10^{-3} mm, and average stresses experienced by the instrument are within 10 MPa, which still has plenty of safety margin (10s of MPa). Using the 3σ rule, where we multiply the average stress by 3, the displacements and stresses are still under the materials' yield strength.

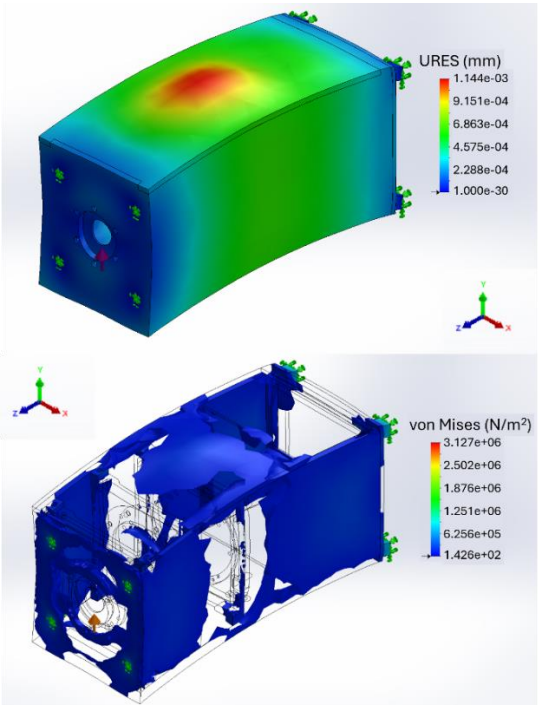

Figure 6 HERT random vibration simulation with Y-axis excitation. (Top) resultant displacement; (bottom) von Mises stress.

SUMMARY

As a miniaturized telescope, HERT meets the instrument requirements for energy resolution based on Geant4 simulations, radiation tolerance based on TID testing, and can survive a vibrational load specified by NASA GEVS 7000 with a significant safety margin based on random vibration simulations. Ongoing bench testing with muons and an SR-90/Y-90 radioactive source and the planned beam testing will further test and verify HERT's performance. Together with environmental testing, HERT will be at TRL 6 and ready for flight at the end of the performance period. With a CubeSat mission at GTO, HERT will provide valuable, high-energy-resolution measurements of radiation belt core electron population and greatly advance the quantitative understanding of radiation belt electron acceleration.

ACKNOWLEDGMENTS

This work is sponsored by NASA Grants 80NSSC21K1041 and 80NSSC24K0740. We thank Lengying Khoo, Vaughn Hoxie, Spencer Boyajian, Ryan Bolin, Charlie Fisher, Michael Fogle, Max Cichon, and Tami Isaacs-Smith for their guidance and help in instrument design, characterization, and testing.

REFERENCES

1. Fälthammar, C.-G. (1965), Effects of time-dependent electric fields on geomagnetically trapped radiation, J. Geophys. Res., 70(11), 2503–2516, doi:10.1029/JZ070i011p02503.
2. Schulz, M., and L. Lanzerotti (1974), Particle Diffusion in the Radiation Belts, pp. 153–159, Springer, New York.
3. Reeves, G. D., Spence, H. E., Henderson, M. G., Morley, S. K., Friedel, R. H. W., Funsten, H. O., et al. (2013). Electron acceleration in the heart of the Van Allen radiation belts. Science, 341(6149), 991–994. https://doi.org/10.1126/science.1237743.
4. Drozdov, A. Y., Blum, L. W., Hartinger, M., Zhao, H., Lejosne, S., Hudson, M. K., et al. (2022). Radial transport versus local acceleration: The longstanding debate. Earth and Space Science, 9, e2022EA002216. https://doi.org/10.1029/2022EA002216.
5. Lejosne S, Allison HJ, Blum LW, Drozdov AY, Hartinger MD, Hudson MK, Jaynes AN, Ozeke L, Roussos E and Zhao H (2022). Differentiating Between the Leading Processes for Electron Radiation Belt Acceleration. Front. Astron. Space Sci. 9:896245. doi: 10.3389/fspas.2022.896245.
6. Sarris, T. E., X., Li, M., Temerin, H. Zhao, S., Califf, W., Liu, and R., Ergun (2017), On the

Relationship Between Electron Flux Oscillations and ULF Wave-Driven Radial Transport, J. Geophys. Res. Space Physics, 122, doi:10.1002/2016JA023741.

7. Sarris, T. E., X. Li, M. A. Temerin, H. Zhao, L.-Y. Khoo, D. L. Turner, W. Liu, and S. G. Claudepierre (2020). Simulations of electron flux oscillations as observed by MagEIS in response to broadband ULF waves, Journal of Geophysical Research: Space Physics, 125, e2020JA027798. https://doi.org/10.1029/2020JA027798.

8. Baker, D. N., Kanekal, S. G., Hoxie, V. C., Batiste, S., Bolton, M., Li, X., et al. (2013). The Relativistic Electron-Proton Telescope (REPT) instrument on board the Radiation Belt Storm Probes (RBSP) spacecraft: Characterization of Earth's radiation belt high-energy particle populations. Space Science Reviews, 179(1-4), 337–381. https://doi.org/10.1007/s11214-012-9950-9.

9. Baker, D. N., Kanekal, S. G., Hoxie, V., Li, X., Jaynes, A. N., Zhao, H., et al. (2021). The relativistic electron-proton telescope (REPT) investigation: Design, operational properties, and science highlights. Space Science Reviews, 217(5), 68. https://doi.org/10.1007/s11214-021-00838-3.

10. Mauk, B., N. Fox, S. Kanekal, R. Kessel, D. Sibeck, and A. Ukhorskiy (2012), Science objectives and rationale for the radiation belt storm probes mission, Space Sci. Rev., 179, 3–27, doi:10.1007/s11214-012-9908-y.

11. Kessel, R. L., N. J. Fox, and M. Weiss (2013), The Radiation Belt Storm Probes (RBSP) and space weather, Space Sci. Rev., 179(1-4), 531–543, doi:10.1007/s11214-012-9953-6.

12. Li, X., et al. (2013), First results from CSSWE CubeSat: Characteristics of relativistic electrons in the near-Earth environment during the October 2012 magnetic storms, J. Geophys. Res. Space Physics, 118, doi:10.1002/2013JA019342.

13. Khoo, L. -Y., Li, X., Selesnick, R. S., Schiller, Q., Zhang, K., Zhao, H., et al. (2022). On the Challenges of Measuring Energetic Particles in the Inner Belt: A Geant4 Simulation of an Energetic Particle Detector Instrument, REPTile-2. Journal of Geophysical Research: Space Physics, 127, e2021JA030249. https://doi.org/10.1029/2021JA030249.

14. Li, X., Selesnick, R., Mei, Y., O'Brien, D., Hogan, B., Xiang, Z., Khoo, L. -Y., Zhao, H., Schiller, Q., Temerin, M., and Baker, D. N. (2024). First results from REPTile-2 measurements onboard CIRBE. Geophysical Research Letters. 51, e2023GL107521. https://doi.org/10.1029/2023GL107521.

15. Li, X., Kohnert, R., Palo, S., Selesnick, R., Khoo, L., & Schiller, Q. (2022). Two generations of CubeSat missions (CSSWE and CIRBE) to take onthe challenges of measuring relativistic electrons in Earth's magnetosphere. In 36th annual small satellite conference. Retrieved from https://digitalcommons.usu.edu/cgi/viewcontent.cgi?article=5311&context=smallsat.

16. Krantz, S. H., Zhao, H., Blum, L. W., Li, X., and Cantilina, J. (2023). Design and Instrument Characterization of the High-Energy Resolution relativistic electron Telescope (HERT) using Geant4 Simulation. Journal of Geophysical Research: Space Physics, 128, e2023JA031632. https://doi.org/10.1029/2023JA031632.